HHS Public Access

Author manuscript

Nat Neurosci. Author manuscript; available in PMC 2013 October 01.

Published in final edited form as:

Nat Neurosci. 2013 April ; 16(4): 473–478. doi:10.1038/nn.3352.

A shared inhibitory circuit for both exogenous and endogenous control of stimulus selection

Shreesh P. Mysore[*] and **Eric I. Knudsen**

299 W. Campus Drive, Department of Neurobiology, Stanford University, Stanford CA 94305, USA

Abstract

The mechanisms by which the brain suppresses distracting stimuli to control the locus of attention are unknown. We found that focal, reversible inactivation of a single inhibitory circuit in the barn owl midbrain tegmentum, the nucleus isthmi pars magnocellularis (Imc), abolished both stimulus-driven (exogenous) and internally-driven (endogenous) competitive interactions in the optic tectum (superior colliculus in mammals), which are vital to the selection of a target among distracters in behaving animals. Imc neurons transformed spatially precise multisensory and endogenous input into powerful inhibitory output that suppressed competing representations across the entire tectal space map. We identified a small, but highly potent, circuit that is employed by both exogenous and endogenous signals to exert competitive suppression in the midbrain selection network. Our findings reveal, for the first time, a neural mechanism for the construction of a priority map that is critical for the selection of the most important stimulus for gaze and attention.

To behave adaptively in a complex environment, an animal must select the most important stimulus at each moment for further neural processing. The selection of the highest priority stimulus for attention is determined by competitive interactions among the neural representations of all stimuli in the environment. Two aspects of each stimulus influence these competitive interactions[1] (see also[2]): (i) its physical properties, such as its intensity, speed of motion or novelty, and (ii) its relevance to the animal's behavior, such as whether the stimulus predicts reward or whether the animal intends to direct its gaze towards the stimulus. The effects of such exogenous and endogenous influences, respectively, on the neural representations of competing stimuli have been studied extensively in both forebrain (fronto-parietal) and midbrain structures involved in the control of attention, with response suppression being a hallmark of these competitive interactions[3–8]. However, the identity of the neurons that actually mediate competitive suppression is not known.

The midbrain selection network, conserved across vertebrate evolution, provides an ideal substrate to search for specific circuits that are involved in stimulus selection[7]. It consists of

[*]Correspondence should be addressed to shreesh@stanford.edu.

Author contributions SPM and EIK designed the research and wrote the paper. SPM performed the experiments and the analyses.

The authors declare that there are no conflicts of interest.

the optic tectum (superior colliculus in mammals), and a number of interconnected tegmental nuclei that contain groups of GABAergic, cholinergic and glutamatergic neurons. In birds, this network achieves its highest degree of differentiation[7], with functionally distinct circuits being spatially segregated, thereby greatly facilitating the ability to access selectively various network components.

A key node in the midbrain selection network is the intermediate and deep layers of the optic tectum (OTid; layers 10–15 in birds; layers 3–7 in mammals), which has been shown to play a critical role in stimulus selection for attention in monkeys[9, 10]. The OTid encodes the relative priorities of stimuli for gaze and attention in a topographic map of space by combining multisensory exogenous signals of physical salience with endogenous signals of behavioral relevance associated with each location[7]. Importantly, both exogenous and endogenous signals associated with a location competitively inhibit OTid responses to stimuli at all other locations[11–14]. This competitive inhibition results in a highly reliable, categorical representation of the locus of the strongest stimulus, a representation that is exceptionally sensitive to the relative priorities of the competing stimuli[13, 15]. Such competitive interactions can account for the correct selection of a target among distracters[16] in behaving monkeys[9, 10, 16].

What circuit mediates competitive inhibition among exogenous signals, and does the same circuit also mediate competitive inhibition of irrelevant locations by endogenous signals[17]? An obvious candidate circuit in the midbrain network is the nucleus isthmi pars magnocellularis (Imc; lateral tegmental nucleus in mammals; Fig. 1a–c and Supp. Fig. 1a). The Imc is composed of GABAergic neurons that interconnect with the OTid[18]. Imc neurons receive a topographic projection from the OTid (layer 10b) and they project back broadly to the OTid space map[18]. The pharmacology and pattern of connectivity suggest that the Imc may be the source of global inhibition in the OTid. Indeed, Imc blockade has been shown to reduce competitive suppression among exogenous signals in a cholinergic component of the midbrain network[19]. Here, we use reversible blockade of synaptic inputs to the Imc in barn owls to examine the role of the Imc in mediating exogenous and endogenous competitive inhibition in the OTid.

RESULTS

We hypothesized that the Imc mediates the competitive inhibition in the OTid that results from both exogenous and endogenous signals. To test this hypothesis, we measured the strength of exogenous and endogenous competitive inhibition in the OTid before, during and after blocking excitatory synaptic transmission in the Imc in head-fixed, non-anesthetized barn owls. Transmission blockade was achieved by focal, iontophoretic application of kynurenic acid, a competitive inhibitor of ionotropic glutamate receptors, delivered through a multi-barreled recording/injection electrode, positioned at specific sites in the Imc space map (Methods).

Role of the Imc in exogenous competitive inhibition

The first set of experiments tested the hypothesis that the Imc circuit mediates stimulus-driven (exogenous) competitive inhibition in the midbrain network. Exogenous, competitive

inhibition in the OTid exhibits several distinctive properties: it operates across the entire space map, it acts independently of the modality of the stimulus, and the strength of the inhibition increases as the strength of the competitor is increased. These properties can only be observed when multiple stimuli are presented to the animal[11, 13]. In our experiments, we measured them by simultaneously presenting two stimuli to the animal: one centered in the receptive field of the OTid unit ("RF stimulus"); the other ("competitor") located far outside of the RF, typically >30° from the RF center. The RF stimulus was always a visual looming dot, and the competitor was either another looming dot or an auditory noise burst (Methods).

We began by measuring the contribution of the Imc to the suppressive effect of a distant competitor on spatial tuning curves in the OTid (Fig. 2a–i). Consistent with previously published results[11], the competing stimulus strongly suppressed OTid unit responses to an RF stimulus (Fig. 2d,g). We then positioned the iontophoretic electrode at the site in the Imc space map that represented the location of the competitor (Fig. 2b). Ejection of kynurenic acid blocked all responses to the competitor at the Imc injection site (Fig. 2j–k). At the same time, it also abolished competitor-mediated inhibition in the OTid (Fig. 2e,h vs. 2d,g). Following cessation of Imc blockade, responses to the competitor in the Imc and competitive inhibition in the OTid both re-appeared (Fig. 2l and 2f,i, respectively). Moreover, responses to RF stimuli presented alone remained unchanged across the three conditions (Fig. 2g vs. 2h vs. 2i; maximum response to RF stimulus alone during baseline vs. Imc blockade: t-test, $t(22) = 2.99$, $p = 0.233$; maximum response to RF stimulus alone during Imc blockade vs. recovery: Wilcoxon ranksum test, $Z = 0.03$, $p = 0.98$).

These effects were verified across a population of 18 OTid units (Fig. 2m–n and Suppl. Fig. 1). Powerful competitive suppression during the baseline condition (Fig. 2m, left column, filled circles: statistically significant suppression) was abolished for the majority of units following Imc blockade (16/18 units; Fig. 2m, middle column, open circles: suppression not significant; Suppl. Fig. 1b, unit-by-unit analysis). Responses to single stimuli, however, remained unaffected for the majority of units (14/18; Suppl. Fig. 1c). The receptive field locations of the tested units and, therefore, the positions of the competitor stimuli, were distributed widely across space (Suppl. Fig. 1d; median distance of competitor from RF center = 43°; median loom speeds = 4 °/s (RF stimulus), 7.2 °/s (competitor)), demonstrating the Imc's role in mediating exogenous suppression across the entire OTid space map. The variability in the strength of competitive suppression in the baseline condition (Fig. 2m, left column) did not correlate with the spatial positions of the competitors ($p > 0.05$, individual factors and two-factor interaction; two-way ANOVA on the percentage of suppression in the baseline condition with azimuthal and elevational distances as factors, $n = 18$ units from 4 birds; azimuth: $F(1, 14) = 0.28$, $p = 0.6$; elevation: $F(1, 14) = 0.38$, $p = 0.55$; interaction: $F(1, 14) = 0.28$, $p = 0.61$). Rather, the variability was consistent with unit-to-unit variability in the strength of competitive suppression, as reported previously[11, 13].

The elimination of competitive inhibition in the OTid by Imc blockade occurred only when the competitor was positioned at the location represented at the site of blockade in the Imc space map. When the competing stimulus was moved away from the locus represented at the Imc inactivation site (median separation = 30°; Suppl. Fig. 2a), but still outside of the OTid RF (Fig. 3a, top panel), Imc blockade had no effect on competitor suppression of OTid

responses (Fig. 3a, bottom panel). This result demonstrates that sensory input to the Imc circuit is spatially precise and that our blockade of Imc drive was focal.

Next, we tested whether the Imc mediates exogenous competitive inhibition across sensory modalities. To address this question, we repeated the first experiment, but replaced the visual competitor with an auditory competitor (Fig. 3b, top panel). The auditory competitor was a broadband noise burst with a median binaural level of 42 dB above unit threshold and located, in dichotic space, 38° ± 2° to the side of the OTid RF center (Suppl. Fig. 2c). The binaural level ("strength") of the auditory competitor was chosen to yield consistently strong competitive inhibition across OTid units, based on results from a previous study[13]. As expected, a distant auditory competitor powerfully suppressed OTid unit responses to the visual RF stimulus (n = 14; Fig. 3b, bottom panel). This cross-modal suppression was, again, drastically reduced by focal blockade at the Imc site that represented the location of the auditory stimulus (Fig. 3b, bottom panel and Suppl. Fig. 2d).

Finally, we tested whether the unusual strength dependence of competitive inhibition in the OTid depends on the Imc[13, 15]. For most units in the OTid, inhibition by a distant competitor increases with the strength of the competitor[13] (the others are not affected by a competitor). Notably, for half of these units the inhibition increases abruptly, in a switch-like manner, when the strength of the competitor exceeds that of the RF stimulus; and for the other half, inhibition increases gradually with the strength of the competitor stimulus. When the responses of switch-like, gradual, and non-suppressed units are examined together, the resulting pattern of population activity exhibits abrupt changes as a function of relative stimulus strength, and categorizes stimuli as "strongest" or "other".

To test the role of the Imc in mediating this competitor strength-dependent inhibition, we measured competitor strength-response profiles without and with Imc blockade (Fig. 4a). For these experiments, the RF stimulus was presented with a fixed strength (average loom speed = 7 °/s ± 0.8 °/s) at the center of the OTid RF, and the distant competitor (median distance from RF center = 42°; Suppl. Fig. 2e) was presented over a range of (interleaved) strengths (Suppl. Fig. 2e and[13]). Imc blockade at the site that represented the location of the competitor abolished the competitor strength-dependent inhibition (Fig. 4b: switch-like; Fig. 4c: gradual): responses to the RF stimulus were no longer correlated with the strength of the competitor, and the maximum suppression (typically caused by the strongest competitor; 17 °/s ± 1 °/s) was not significantly different from zero. These effects were verified across a population of OTid units (n = 12 units; 7-switch-like and 5-gradual; Fig. 4d–f and Suppl. Fig. 2f). Thus, the Imc mediates competitor strength-dependent, exogenous inhibition in the OTid, and is, thereby, necessary for constructing a categorical representation of the strongest stimulus in the OTid.

Role of the Imc in endogenous competitive inhibition

Next, we tested the hypothesis that the Imc circuit also mediates the competitive inhibition that is associated with endogenous signals. To evoke space-specific endogenous signals, we applied sub-saccadic electrical microstimulation (currents weaker than those necessary to elicit eye movements; < 30 μA), to the forebrain gaze control area, called the arcopallial gaze field (AGF). The AGF shares many properties with the mammalian frontal eye field

(FEF): similar patterns of anatomical projections to sensorimotor and premotor structures[20, 21]; necessary role in working memory-dependent gaze control[22, 23]; changes in gaze direction caused by electrical microstimulation[20, 24], and space-specific modulation of sensory neural responses caused by sub-saccadic electrical microstimulation[12, 25]. In monkeys, such sub-saccadic microstimulation of the FEF evokes an endogenous signal that shifts spatial attention covertly to the locus encoded at the FEF stimulation site[26].

We applied sub-saccadic electrical microstimulation to the AGF while monitoring OTid responses to sensory stimuli. For these experiments, we chose OTid sites that encoded locations that were distant from the one encoded by the AGF site ("non-aligned" OTid sites; Fig. 5a–c; average distance between OTid and AGF RFs = 34° ± 3.3°; Suppl. Fig. 3g). Consistent with previously published results[12], we found that AGF microstimulation produced a suppression of responses of non-aligned OTid units to sensory stimuli, with response suppression occurring predominantly at stimulus locations that were either at or near the center of the OTid RF (Fig. 5d and Suppl. Fig. 3d). We then positioned the iontophoresis electrode at the site in the Imc space map that encoded the same location as the AGF microstimulation site ("aligned" site; average distance between RFs = 2.2° ± 0.3°). Blockade of responses at the Imc site aligned with the AGF stimulation site completely abolished endogenous competitive inhibition (Fig. 5e and Suppl. Fig. 3e), and cessation of drug application resulted in recovery of endogenous inhibition in the OTid (Fig. 5f and Suppl. Fig. 3f). This result was confirmed across a population of 14 OTid units, for which the site of Imc blockade was aligned with the AGF microstimulation site (Fig. 5g and Suppl. Fig. 3h). Note that, in this protocol, the endogenous signal encoded a location at which no stimulus was present[12, 27, 28]. This protocol is ideal for the purposes of isolating the neural circuits responsible for endogenous inhibition: the absence of a stimulus at the location encoded by the microstimulation site eliminates the explicit contribution of stimulus-driven, exogenous competitive inhibition.

In other experiments, the Imc was blocked at sites that were non-aligned with both the AGF microstimulation site (average distance between RFs = 35° ± 7.1°) and the OTid unit RF (average distance = 42° ± 6.5 °; Fig. 6a, top panel and Suppl. Fig. 4a). In this configuration, Imc blockade had no effect on endogenous competitive inhibition in the OTid (Fig. 6a, bottom panel), demonstrating the spatial specificity of the effects of Imc blockade on endogenous competitive inhibition (consistent with the effects of Imc blockade on exogenous competitive inhibition; Fig. 3a).

In a final set of experiments, we tested whether endogenous competitive inhibition of auditory responses also depended on the Imc circuit. In this protocol, we repeated the same experiment as described above, but we replaced the visual RF stimulus with an auditory RF stimulus (Fig. 6b, top panel and Suppl. Fig. 4c). AGF microstimulation suppressed auditory responses at non-aligned sites in the OTid space map (Fig. 6b, bottom panel, left column). Upon Imc blockade at a site aligned with the AGF stimulation site, the endogenous inhibition of auditory responses in the OTid was eliminated (Fig. 6b, bottom panel, middle column and Suppl. Fig. 4d). Taken together, these results demonstrate that the Imc is required for generating competitive inhibition among both endogenous and exogenous signals in the OTid.

DISCUSSION

This study demonstrates that a single, shared circuit in the midbrain selection network mediates competitive inhibition among both exogenous and endogenous signals. Global competitive inhibition caused by physically salient stimuli (exogenous competitive inhibition) has been reported for several brain areas, including prefrontal, parietal and extrastriate cortices in mammals[29–32] and in the optic tectum/superior colliculus of many species[16]. In addition, suppression of neural responses to taskirrelevant stimuli (endogenous competitive inhibition) has been documented in a similarly wide range of brain areas, mostly in primate species[17, 33, 34]. However, the Imc is the first circuit to be identified as mediating this critical function. The degree to which activity that is generated in the midbrain network modulates sensory responses in other brain areas remains to be determined.

We have shown that the small population of GABAergic Imc neurons (< 4 % of the number of cells in layer 13 of the optic tectum; Methods) control competitive interactions across the entire OTid space map. By mediating this function across both exogenous and endogenous signals, the effect of the Imc circuit is to render a representation of stimulus priority in the OTid. Moreover, because of switch-like competitive inhibition, the Imc circuit creates a categorical representation of the highest priority stimulus in the OTid, one that is exquisitely sensitive to the difference between the strengths of multiple competing stimuli. The observation that inactivation of the superior colliculus severely impairs the ability of monkeys to select a stimulus either for gaze or attention particularly when a stimulus is in the presence of similar stimuli[9, 10, 35, 36], suggests that the midbrain network, and specifically the Imc (or its homolog in mammals), plays a critical role under these conditions. It will be important to assay the effect of inactivating the Imc or its analog[7] in animals that must select a target from among similar distracters.

Given the essential role of the Imc in competitive inhibition in the midbrain network, several important questions remain to be answered regarding the routing of information through the network. First, how do endogenous signals from the AGF activate the Imc? To date, the only known anatomical input to the Imc originates from the optic tectum[18]. Endogenous signals could be routed to the Imc via the optic tectum or via an as yet undiscovered descending pathway. Second, what is the route by which Imc output suppresses neural responses in the OTid? This could be accomplished either directly, via the projections from the Imc to the OTid, and/or indirectly, via projections from the Imc to the nucleus isthmi pars parvocellularis (Ipc), a cholinergic nucleus with point-to-point, recurrent connections with the optic tectum. Imc inhibition of Ipc activity would reduce any amplifying effect that the Ipc may have on tectal unit responses[37]. The relative importance of these two pathways for OTid suppression needs to be examined. Finally, how do competitive signals in one brain hemisphere reach the opposite hemisphere? In this study, both the exogenous and endogenous competitive signals were selected to correspond to locations that were explicitly represented on the same side of the brain as the RF stimulus (Suppl. Figs. 1–4). However, we have shown previously that stimulus locations that are explicitly represented only in opposite hemispheres can still be mutually inhibitory[11]. Whether cross-hemispheric inhibition is also mediated by the Imc remains an intriguing, unanswered question.

Circuit-level models of the modulation of cortical activity by attention have proposed that endogenous signals modulate neural responses by operating through the same neural mechanisms that govern exogenous stimulus interactions[38–40]. The results from this study provide direct evidence in support of this hypothesis. Inhibitory circuits that act globally across spatial locations, like the Imc, could explain interactions observed in the forebrain between remote stimuli competing for attention[39]. Moreover, Imc-like circuits acting "globally" across feature values (e.g., orientation of visual contours, colors, etc) could account for many of the local, normalizing sensory interactions and the effects of endogenous attention on feature processing that have been reported in forebrain networks[39, 41].

Numerous studies in monkeys and humans have established that neural responses to a sensory stimulus are stronger when an animal attends to the location of a stimulus than when it attends away from that location[33, 42, 43]. Recent neuroimaging results from humans engaged in endogenous control of attention have suggested that these attention-dependent changes in neural responsiveness involve two distinct processes[44]: one that increases neural responses to the attended stimulus (focally) and another that suppresses neural responses to irrelevant information (globally). In support of distinct processes for enhancement and suppression, neurophysiological data from the owl midbrain selection network has shown that space-specific endogenous signals generate simultaneously both focal enhancement of sensory responses to stimuli at the corresponding location in the OTid space map and global suppression of sensory responses to stimuli at all other locations[45]. In this study, we demonstrate that the Imc contributes to global suppression. What circuits might underlie focal enhancement? In the avian midbrain network, the cholinergic Ipc with its recurrent connectivity with the optic tectum stands out as an excellent candidate. It will be important to determine whether the Ipc is, indeed, involved in focal response enhancement in the midbrain, what circuits might serve this function in the forebrain, and whether focal enhancing circuits are also shared by both exogenous and endogenous signals.

METHODS

Animals

Experiments were performed on 9 head-fixed, non-anesthetized, adult barn owls (*Tyto alba)*. Both male and female birds were used. All procedures for bird care and use were approved by the Stanford University Institutional Animal Care and Use Committee and were in accordance with the National Institutes of Health and the Society for Neuroscience guidelines for the care and use of laboratory animals. Owls were group housed in enclosures within the vivarium, each containing 3–5 birds. The light/dark cycle was 12 hrs/12 hrs.

Neurophysiology

Experiments were performed following protocols that have been described previously[11, 13, 46]; Briefly, epoxy-coated tungsten microelectrodes (A-M Systems, 250μm, 5 MOhms at 1 kHz) were used to record single and multi-units extracellularly. A mixture of isofluorane (1.5–2%) and nitrous oxide/oxygen (45:55 by volume) was used at the start of the experiment to anesthetize the bird and secure it in the experimental rig (a 20 minute

period of initial set-up). Isofluorane was turned off immediately after the bird was secured and was never turned back on for the remainder of the experiment. Frequently, nitrous oxide was also turned off at this point, but in several experiments, it was left on for a few hours if the bird's temperament necessitated it (some birds were calm when restrained, while others were not). However, it was turned off at least 30 minutes before the recording session. Our recordings were performed between 10 to 20 hours after initial set-up (the time required for positioning the electrodes). Since recovery from isofluorane occurs well under 30 minutes after it is turned off, and recovery from nitrous oxide occurs within a minute (the bird stands up and flies away if freed from restraints), recordings were made in animals that were not anesthetized.

Multi-unit spike waveforms were sorted off-line into putative single units, as described previously[13]. All recordings in the optic tectum were made in layers 11–13 of the optic tectum (OTid). Visual and auditory stimuli used here have been previously described[11, 13]. Briefly, looming stimuli were dots that expanded linearly in size over time, starting from a size of 0.6° in radius. Visual stimuli were presented on a tangent screen in front of the owl. Auditory stimuli, delivered dichotically through matched earphones, were presented as though from different locations by filtering sounds with headrelated transfer functions[47]. The average binaural levels (referred to also as sound levels) of auditory stimuli are indicated in all Figures relative to the minimum threshold, averaged across units. The levels ("strengths") of the auditory competitors were chosen to achieve powerful, significant suppression of responses to the visual, looming RF stimulus (Fig. 3b; based on previous investigations[13]). No attempt was made to match the strengths of auditory competitors (used for Fig. 3b) with those of the visual competitors (used in Fig. 2) because such matching was not relevant to the question being asked. It was only important that the competitors be effective in suppressing responses to the RF stimuli.

In Figures 2,3,5 and 6, each RF stimulus location was repeatedly tested 10–15 times in a randomly interleaved fashion. Similarly, in Figure 4, each competitor strength value was repeatedly tested 10–15 times in a randomly interleaved fashion.

Iontophoretic blockade

Focal, reversible blockade of excitatory transmission was achieved by iontophoresing a fast onset/offset, pan glutamate receptor antagonist kynurenic acid (SIGMA; 40 mM, 8.5–9 pH), contained in one of the barrels of a three-barrel glass electrode (FHC, 3 barrel borosilicate capillary tubing, 1.2 or 1.5mm OD for each barrel; tip diameter = 25–30 μm for all three barrels together). Ejection was achieved by passing approximately −500nA through the drug barrel using a DAGAN 6400Adv iontophoresis amplifier. Data in the inactivation and recovery conditions were recorded, respectively, after waiting for 5 to 10 minutes after drug ejection started, or after drug ejection ceased (by setting the retaining current to +15 nA). In all cases, the effects of drug onset/offset were verified by examining the responses of the Imc neurons at the site of inactivation. These responses were recorded using one of the other barrels of the glass electrode, which contained a carbon fiber and was saline-filled; the third barrel (also saline-filled; SUM channel) was used to balance the charge delivered by the kynurenic acid-containing barrel.

Upon delivery of kynurenic acid to the Imc, stimulus driven activity at that Imc site was almost completely abolished (Fig. 2n). This was further verified in a subset of sites by measuring responses to increasing strengths (loom speeds) of the competitor stimulus in the three conditions (data not shown). In some cases (about 25%), the delivery of kynurenic acid resulted in the appearance of a large number of spikes that could not be driven by the competitor stimulus. These stimulus-insensitive spikes disappeared once the delivery of kynurenic acid ceased. Since the Imc is replete with fibers of passage, and Imc neurons are thought to be mutually inhibitory[18, 46], this increase in the number of stimulus-insensitive spikes measured at the inactivated site is best explained as the increased activity of fibers of passage from other Imc neurons that have been disinhibited due to synaptic blockade at the inactivated site.

AGF microstimulation

Electrical microstimulation of the AGF was achieved following the protocol described previously[12, 48]. Briefly, an epoxy-coated tungsten microelectrode (FHC; 1 MOhm at 1kHz) was used to identify a “patch” of tissue in the AGF with consistent spatial tuning. This was defined as a 300 μm span along the dorsoventral penetration path of the electrode, such that the locations of unit visual receptive fields measured at the top, middle and bottom of the span were not significantly different (centered within ± 5 °). Electrical stimulation consisted of biphasic 200 Hz pulses, delivered for 25 ms (Grass S88 stimulator with two Grass stimulus isolation units PSIU-6). AGF stimulation was delivered starting at 0 ms (i.e., simultaneously with stimulus onset) when the RF stimulus in the OTid RF was visual, and at −25 ms (25 ms before stimulus onset) when the RF stimulus was auditory. Current levels (5–25 μA) were far below those required to elicit small amplitude eye deflections (100–600 μA); current amplitudes were measured from the voltage drop across a 1 kOhm resistor in the return path of the current source.

Data analysis and statistical methods

All analyses were carried out with custom MATLAB code. The spatial receptive field for each unit was defined as the set of locations at which a single stimulus evoked responses above baseline. The receptive field locations of the recorded units in the OTid, Imc, and AGF are shown for each set of experiments in Supplementary Figures 1c, 2a,c,e, 3g, and 4a,c. Note that in the barn owl, the OTid in each hemisphere represents locations from up to 15° into ipsilateral space (−15°) through 60° into contralateral space (+60°).

Response firing rates were computed by counting spikes over a time window and converting the resulting count into spikes per second. The optimal window for each unit was defined as the time between the first instant at which the inhibition was statistically significant, and the last instant at which it was statistically significant, after rounding off both values to the nearest multiple of 10 ms. Statistical significance was determined as described previously[13]. Briefly, we compared the average instantaneous firing rates obtained with the RF stimulus alone versus with both the RF stimulus and a competitor/AGF stimulation using a running ANOVA and an empirical criterion for significant difference at the 0.05 level[13]. For Figures 2 and 3a, the median start and end times of the windows were [50 ms, 300 ms], respectively, with stimulus onset occurring at 0 ms. The median count windows for the other

experimental tests were [0 ms, 300 ms] (Figs. 3b, 4b–f), [110 ms, 310 ms] (Fig. 5), [150 ms, 320 ms] (Fig. 6a), and [50 ms, 230 ms] (Fig. 6b). The differences in the windows reflected a combination of unit-to-unit variability in the onset and duration of inhibition, as well as the source-dependence of the inhibitory signal (inhibition due to a visual versus an auditory stimulus, or an endogenous signal).

Parametric or non-parametric, paired statistical tests were applied based on whether the distributions being compared were Gaussian or not (Lilliefors test of normality); tests were always two-tailed. The Holm-Bonferroni correction for multiple comparisons was applied when appropriate by including only those comparisons that were individually significant. Data shown as a ± b refer to mean ± s.e.m. The '*' symbol indicates significance at the 0.05 level. In statistically comparing the data across the three experimental conditions (baseline, Imc blockade, and recovery), the experimenter was not blind to the experimental conditions to which the data sets belonged.

Correlations between responses to paired stimuli and the strength of the competitor stimulus were tested using Spearman's rank correlation coefficient (*corr* command in MATLAB with the Spearman option).

The transition range of a competitor strength-response profile was defined as the range of competitor strengths over which responses dropped from 90% to 10% of the total range of responses[13]. The range of responses was estimated by fitting sigmoidal functions to the data, and using the fits to determine the minimum and maximum response levels over a standard range of loom-speeds (0 °/s to 22 °/s). Switch-like response profiles were defined as those for which the transition range was ≤ 4°/s[13].

The OTid is approximately 6 mm rostrocaudally and 4.1 mm dorsoventrally, after accounting for curvature. In contrast, the Imc is only 2.8 mm rostrocaudally and 0.35 mm dorsoventrally, appearing as a 700 μm × 350 μm elliptical disk in transverse sections (shown here). The numbers of cells in the Imc and layer 13 of the optic tectum were estimated by counting cell bodies in seven representative Nissl sections, and using the counts to calculate the total number of cells over the entire volumes of these structures.

Replicability

As demonstrated by the summary data in Figures 2–6, the experiments were all repeatable. However, because of the complexity of the design of the experiment in Figures 5 and 6 (involving precise positioning of three electrodes, including one three-barrel glass electrode), and the length of each experiment (frequently >15 hours), only about 40% of these experiments were successful. In the remaining attempts, the experiments were terminated after 15 hours if data collection within a few hours did not appear feasible.

Supplementary Material

Refer to Web version on PubMed Central for supplementary material.

Acknowledgements

This work was supported by funding from the NIH (9R01 EY019179, EIK). We thank Phyllis Knudsen for the immunohistochemistry. We are grateful to Ali Asadollahi, Astra Bryant, Alex Goddard, Jason Schwarz and Nick Steinmetz for critically reading the manuscript.

REFERENCES

1. Fecteau JH, Munoz DP. Salience, relevance, and firing: a priority map for target selection. Trends Cogn Sci. 2006; 10:382–390. [PubMed: 16843702]
2. Awh E, Belopolsky AV, Theeuwes J. Top-down versus bottom-up attentional control: a failed theoretical dichotomy. Trends Cogn Sci. 2012; 16:437–443. [PubMed: 22795563]
3. Reynolds JH, Chelazzi L. Attentional modulation of visual processing. Annu Rev Neurosci. 2004; 27:611–647. [PubMed: 15217345]
4. Bisley JW. The neural basis of visual attention. J Physiol. 2010; 589:49–57. [PubMed: 20807786]
5. Gazzaley A, Cooney JW, Rissman J, D'Esposito M. Top-down suppression deficit underlies working memory impairment in normal aging. Nat Neurosci. 2005; 8:1298–1300. [PubMed: 16158065]
6. McMains S, Kastner S. Interactions of top-down and bottom-up mechanisms in human visual cortex. J Neurosci. 2011; 31:587–597. [PubMed: 21228167]
7. Knudsen E. Control form below: The contribution of a midbrain network to spatial attention. European Journal of Neuroscience. 2011; 33:1961–1972. [PubMed: 21645092]
8. Zanto TP, Gazzaley A. Neural suppression of irrelevant information underlies optimal working memory performance. J Neurosci. 2009; 29:3059–3066. [PubMed: 19279242]
9. Lovejoy LP, Krauzlis RJ. Inactivation of primate superior colliculus impairs covert selection of signals for perceptual judgments. Nat Neurosci. 2010; 13:261–266. [PubMed: 20023651]
10. McPeek RM, Keller EL. Deficits in saccade target selection after inactivation of superior colliculus. Nat Neurosci. 2004; 7:757–763. [PubMed: 15195099]
11. Mysore SP, Asadollahi A, Knudsen EI. Global inhibition and stimulus competition in the owl optic tectum. J Neurosci. 2010; 30:1727–1738. [PubMed: 20130182]
12. Winkowski DE, Knudsen EI. Top-down gain control of the auditory space map by gaze control circuitry in the barn owl. Nature. 2006; 439:336–339. [PubMed: 16421572]
13. Mysore SP, Asadollahi A, Knudsen EI. Signaling of the strongest stimulus in the owl optic tectum. J Neurosci. 2011; 31:5186–5196. [PubMed: 21471353]
14. Basso MA, Wurtz RH. Modulation of neuronal activity by target uncertainty. Nature. 1997; 389:66–69. [PubMed: 9288967]
15. Mysore SP, Knudsen EI. Flexible categorization of relative stimulus strength by the optic tectum. J Neurosci. 2011; 31:7745–7752. [PubMed: 21613487]
16. Mysore SP, Knudsen EI. The role of a midbrain network in competitive stimulus selection. Curr Opin Neurobiol. 2011; 21:653–660. [PubMed: 21696945]
17. Carrasco M. Covert attention increases contrast sensitivity: Psychophysical, neurophysiological and neuroimaging studies. Prog Brain Res. 2006; 154:33–70. [PubMed: 17010702]
18. Wang Y, Major DE, Karten HJ. Morphology and connections of nucleus isthmi pars magnocellularis in chicks (Gallus gallus). J Comp Neurol. 2004; 469:275–297. [PubMed: 14694539]
19. Marin G, et al. A cholinergic gating mechanism controlled by competitive interactions in the optic tectum of the pigeon. J Neurosci. 2007; 27:8112–8121. [PubMed: 17652602]
20. Knudsen EI, Cohen YE, Masino T. Characterization of a forebrain gaze field in the archistriatum of the barn owl: microstimulation and anatomical connections. J Neurosci. 1995; 15:5139–5151. [PubMed: 7623141]
21. Stanton GB, Goldberg ME, Bruce CJ. Frontal eye field efferents in the macaque monkey: II. Topography of terminal fields in midbrain and pons. J Comp Neurol. 1988; 271:493–506. [PubMed: 2454971]

22. Knudsen EI, Knudsen PF. Disruption of auditory spatial working memory by inactivation of the forebrain archistriatum in barn owls. Nature. 1996; 383:428–431. [PubMed: 8837773]
23. Dias EC, Segraves MA. Muscimol-induced inactivation of monkey frontal eye field: effects on visually and memory-guided saccades. J Neurophysiol. 1999; 81:2191–2214. [PubMed: 10322059]
24. Bruce CJ, Goldberg ME, Bushnell MC, Stanton GB. Primate frontal eye fields. II. Physiological and anatomical correlates of electrically evoked eye movements. J Neurophysiol. 1985; 54:714–734. [PubMed: 4045546]
25. Moore T, Armstrong KM. Selective gating of visual signals by microstimulation of frontal cortex. Nature. 2003; 421:370–373. [PubMed: 12540901]
26. Moore T, Fallah M. Control of eye movements and spatial attention. Proc Natl Acad Sci U S A. 2001; 98:1273–1276. [PubMed: 11158629]
27. Sundberg KA, Mitchell JF, Reynolds JH. Spatial attention modulates center-surround interactions in macaque visual area v4. Neuron. 2009; 61:952–963. [PubMed: 19324003]
28. Kastner S, Pinsk MA, De Weerd P, Desimone R, Ungerleider LG. Increased activity in human visual cortex during directed attention in the absence of visual stimulation. Neuron. 1999; 22:751–761. [PubMed: 10230795]
29. Falkner AL, Krishna BS, Goldberg ME. Surround suppression sharpens the priority map in the lateral intraparietal area. J Neurosci. 2010; 30:12787–12797. [PubMed: 20861383]
30. Bair W, Cavanaugh JR, Movshon JA. Time course and time-distance relationships for surround suppression in macaque V1 neurons. J Neurosci. 2003; 23:7690–7701. [PubMed: 12930809]
31. Schall JD, Hanes DP, Thompson KG, King DJ. Saccade target selection in frontal eye field of macaque. I. Visual and premovement activation. J Neurosci. 1995; 15:6905–6918. [PubMed: 7472447]
32. Desimone R, Moran J, Schein SJ, Mishkin M. A role for the corpus callosum in visual area V4 of the macaque. Vis Neurosci. 1993; 10:159–171. [PubMed: 8424923]
33. Desimone R, Duncan J. Neural mechanisms of selective visual attention. Annu Rev Neurosci. 1995; 18:193–222. [PubMed: 7605061]
34. Knudsen EI. Fundamental components of attention. Annu Rev Neurosci. 2007; 30:57–78. [PubMed: 17417935]
35. Nummela SU, Krauzlis RJ. Inactivation of primate superior colliculus biases target choice for smooth pursuit, saccades, and button press responses. J Neurophysiol. 2010; 104:1538–1548. [PubMed: 20660420]
36. Zenon A, Krauzlis RJ. Attention deficits without cortical neuronal deficits. Nature. 2012; 489:434–437. [PubMed: 22972195]
37. Marin G, Mpodozis J, Sentis E, Ossandon T, Letelier JC. Oscillatory bursts in the optic tectum of birds represent re-entrant signals from the nucleus isthmi pars parvocellularis. J Neurosci. 2005; 25:7081–7089. [PubMed: 16049185]
38. Lee DK, Itti L, Koch C, Braun J. Attention activates winner-take-all competition among visual filters. Nat Neurosci. 1999; 2:375–381. [PubMed: 10204546]
39. Reynolds JH, Heeger DJ. The normalization model of attention. Neuron. 2009; 61:168–185. [PubMed: 19186161]
40. Lee J, Maunsell JH. A normalization model of attentional modulation of single unit responses. PLoS One. 2009; 4:e4651. [PubMed: 19247494]
41. Cavanaugh JR, Bair W, Movshon JA. Nature and interaction of signals from the receptive field center and surround in macaque V1 neurons. J Neurophysiol. 2002; 88:2530–2546. [PubMed: 12424292]
42. Kastner S, Ungerleider LG. Mechanisms of visual attention in the human cortex. Annu Rev Neurosci. 2000; 23:315–341. [PubMed: 10845067]
43. Carrasco M. Visual attention: the past 25 years. Vision Res. 2011; 51:1484–1525. [PubMed: 21549742]

44. Gazzaley A, Cooney JW, McEvoy K, Knight RT, D'Esposito M. Top-down enhancement and suppression of the magnitude and speed of neural activity. J Cogn Neurosci. 2005; 17:507–517. [PubMed: 15814009]

45. Winkowski DE, Knudsen EI. Distinct mechanisms for top-down control of neural gain and sensitivity in the owl optic tectum. Neuron. 2008; 60:698–708. [PubMed: 19038225]

46. Mysore SP, Knudsen EI. Reciprocal inhibition of inhibition: a circuit motif for flexible categorization in stimulus selection. Neuron. 2012; 73:193–205. [PubMed: 22243757]

47. Witten IB, Knudsen PF, Knudsen EI. A dominance hierarchy of auditory spatial cues in barn owls. PLoS One. 2010; 5:e10396. [PubMed: 20442852]

48. Winkowski DE, Knudsen EI. Top-down control of multimodal sensitivity in the barn owl optic tectum. J Neurosci. 2007; 27:13279–13291. [PubMed: 18045922]

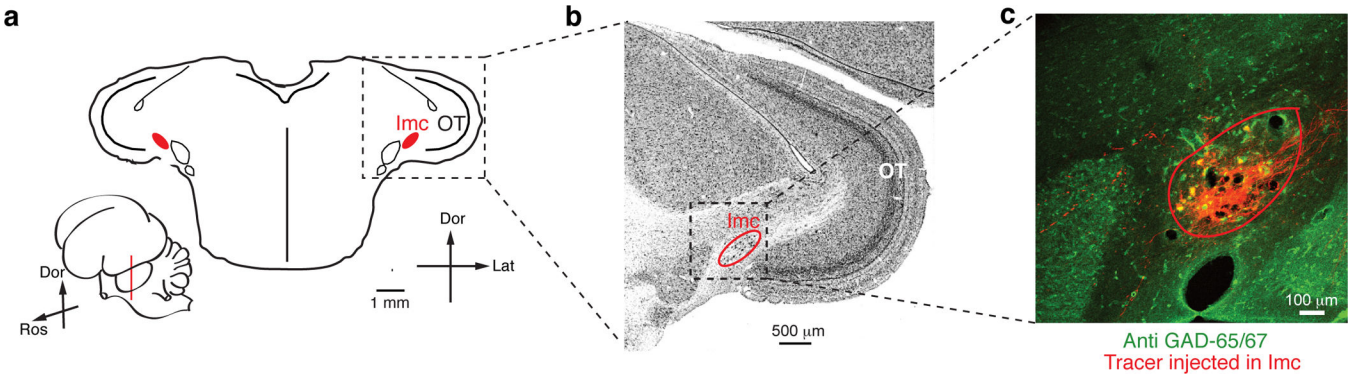

Figure 1. Anatomy of the Imc and optic tectum

(a) *Inset.* Cartoon showing owl brain and plane of section. Transverse section of owl midbrain showing the optic tectum and the Imc. (b) Nissl stain of the boxed region from a. The optic tectum is the C-shaped, multilayered structure that wraps around the Imc; layer 1 is the outermost layer, and layer numbers increase radially inward; layer 10 is the darkly stained band of cell bodies (indicated in a). (c) Fluorescent image of a transverse midbrain section from an owl in which a fluorescent tracer (dextran tetramethyl rhodamine; in red) was injected iontophoretically into the Imc. The section is also stained for GAD-65/67, a marker for inhibitory neurons (green). Yellow somata indicate double labeled (red + green) Imc neurons; note the sparseness of Imc neurons.

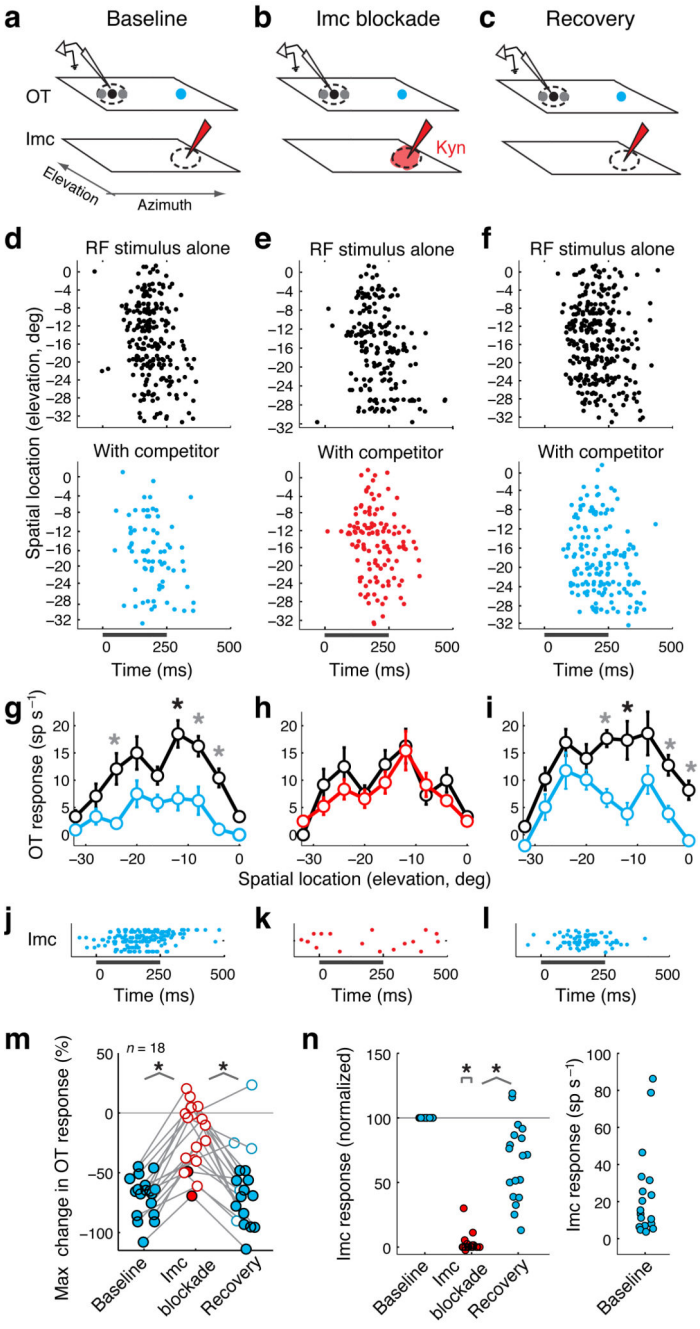

Figure 2. Exogenous competitive inhibition in the OTid abolished by Imc blockade

(a–c) Schematics of electrode configurations for baseline, Imc blockade and recovery conditions. Illustrated are the space maps encoded in the OTid and Imc, receptive fields (dashed ovals: RFs), locations of visual stimuli (black and gray dots: RF stimulus; blue dot: competitor), and electrodes (recording in the OTid; recording/iontophoresis in the Imc). Dot size indicates strength of the stimulus; competitor was always stronger than RF stimulus. (b) Red shading indicates drug being ejected; kyn – kynurenic acid.

(d–f) Rasters of spike responses of an OTid unit to the RF stimulus alone (top panels), or to the RF stimulus and distant competitor (bottom panels). Bar: stimulus duration. Distance between the OTid RF and the location of the competitor (also the site of Imc inactivation) = 33°. Loom speeds: RF stimulus = 4 °/s, competitor = 7.2 °/s.

(g–i) Responses of the OTid unit to the RF stimulus alone (black), or to the RF stimulus and distant competitor (blue/red). Data represent mean ± s.e.m. '*': $p < 0.05$, t-tests at individual locations followed by Holm-Bonferroni correction ($n = 12$ reps per stimulus condition per location, $df = 22$; Methods); black '*': maximum suppression.

(j–l) Rasters of Imc unit responses to the competitor stimulus at the site of drug injection. Dots represent individual spikes, and rows, different stimulus repetitions.

(m) Population summary of maximum response suppression of OTid units (circles) by a distant competitor. Maximum suppression for each unit typically occurred at or near the unit's RF center. Filled circle: maximum suppression was significant ($p< 0.05$; tested as in g), open circle: not significant ($p > 0.05$; as in h). Grey line: connects responses of one unit across conditions. Horizontal spread of points within each condition: random jitter to improve visualization of individual points. '*': $p < 0.05$ (paired Wilcoxon sign rank tests followed by Holm-Bonferroni correction): baseline vs. blockade, $Z = -3.72$, $p = 2*10^{-4}$; blockade vs. recovery, $Z = -3.42$, $p = 6*10^{-4}$; $n = 18$ units from 4 birds. See also Supplementary Figure 1a,b.

(n) Population summary of Imc unit responses to the competitor at the site of blockade. *Left panel:* Response normalized by firing rate in the baseline condition. '*': $p < 0.05$: blockade vs. 100, Wilcoxon sign rank test, $Z = -3.82$, $p = 1*10^{-4}$; blockade vs. recovery; paired Wilcoxon sign rank test, $Z = -3.72$, $p = 2*10^{-4}$; $n = 18$ units from 4 birds. *Right panel:* Absolute firing rates of Imc units.

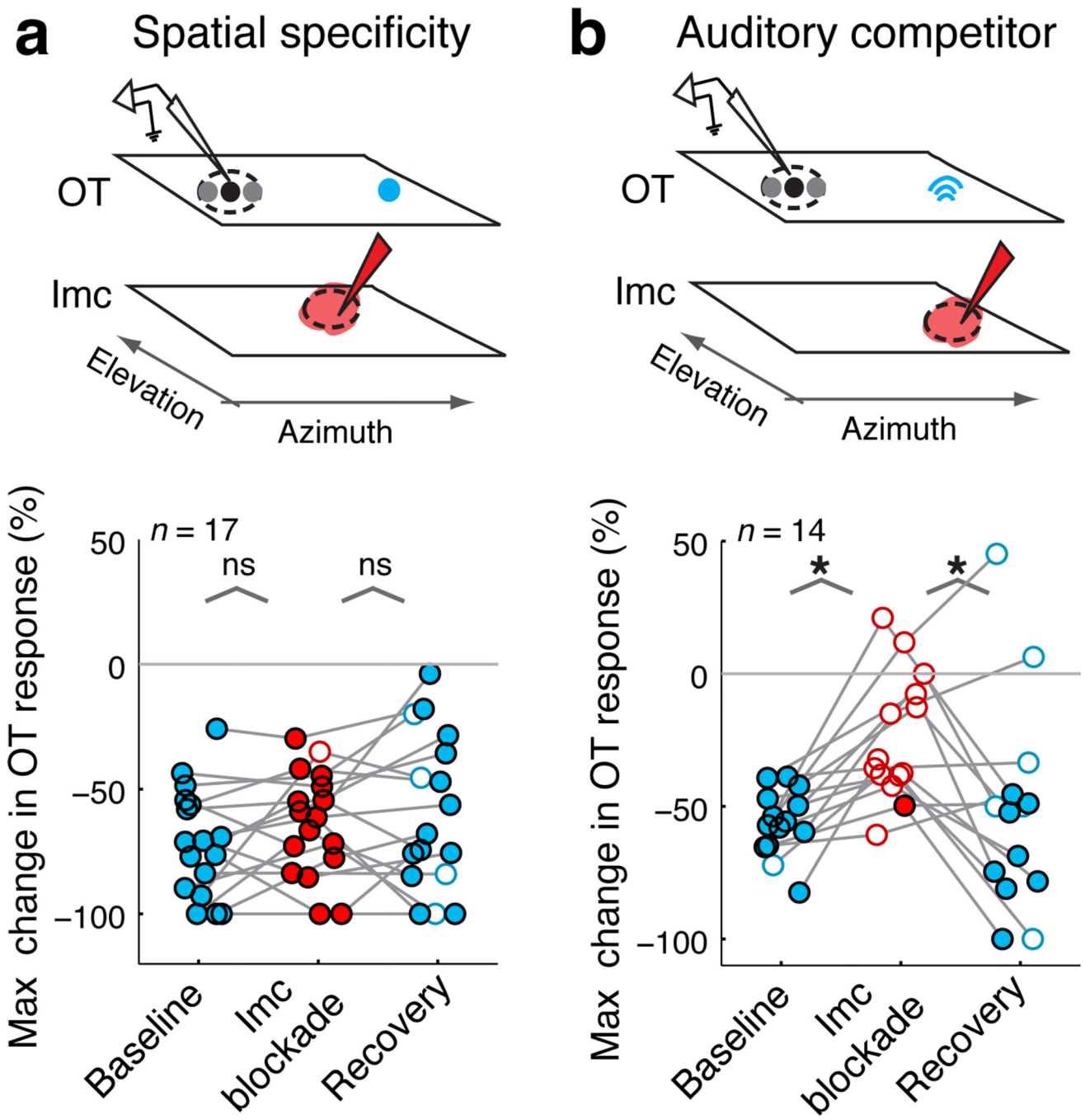

Figure 3. The Imc mediates space-specific, sensory modality independent and switch-like exogenous competitive inhibition in the OTid

(a) Spatial specificity. *Top panel.* The competitor stimulus was located outside both the OTid and Imc RFs. *Bottom panel*. Population summary of competitive suppression of OTid unit responses; same conventions as in Figure 2m; 'ns': $p > 0.05$ (paired t-tests): baseline vs. blockade, $t(16) = -1.58$, $p = 0.14$; blockade vs. recovery, $t(16) = -0.65$, $p = 0.52$; $n = 17$ units from 4 birds.

(b) Sensory modality independence. *Top panel.* Blue icon denotes an auditory competitor stimulus. *Bottom panel*. Population summary of the competitive suppression of OTid unit responses; same conventions as in Figure 2m; '*': $p < 0.05$ (paired t-tests followed by Holm-Bonferroni correction): baseline vs. blockade, $t(13) = -4.45$, $p = 0.0007$; blockade vs. recovery, $t(13) = 2.89$, $p = 0.013$; $n = 14$ units from 4 birds. See also Supplementary Figure 2d.

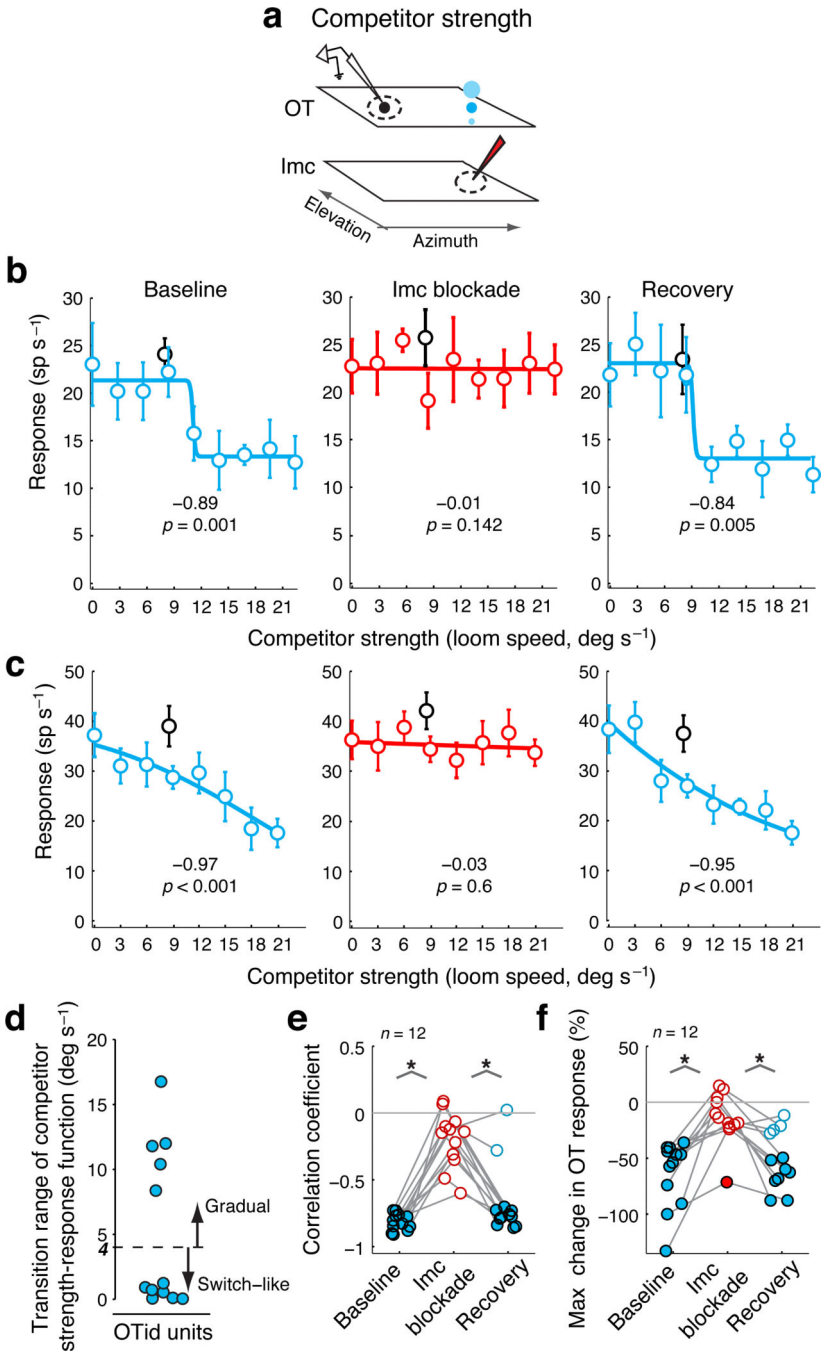

Figure 4. The Imc mediates competitor strength-dependent exogenous inhibition in the OTid

(a) Measurement of competitor strength-dependent response profiles. The strength of the competitor stimulus was systematically increased (blue dots of increasing sizes) while that of the RF stimulus was maintained constant (black dot); same conventions as in 2a–c. (b) Abrupt, switch-like increase in the suppression of an OTid unit's responses as competitor strength increased. Transition range (Methods) = 0.6°/s (left panel). Data in black show responses to RF stimulus alone. Correlation coefficients (response vs. competitor strength) are indicated (Spearman test).

(c) Gradual increase in the suppression of a different OTid unit's responses as competitor strength increased (Methods); transition range = 16.8 °/s (left panel).
(d) Distribution of transition ranges of competitor strength-dependent response profiles measured as in (a); Methods. Using the previously published criterion[13] for identifying switch-like versus gradual response profiles (a transition range cut off of 4°/s), 7/12 CRPs were switch-like and 5/12 were gradual.
(e) Population summary of competitive response correlation coefficient. Same conventions as in 2m. '*': $p < 0.05$ (paired t-tests followed by Holm-Bonferroni correction): baseline vs. blockade, $t(11) = -9.6$, $p < 0.0001$; blockade vs. recovery, $t(11) = 5.4$, $p = 0.0002$; $n = 12$ units from 6 birds (7, with switch-like increase in suppression, and 5, gradual[13]). See also Supplementary Figure 2f.
(f) Population summary of maximum suppression for same units. '*': $p < 0.05$ (paired Wilcoxon rank sum tests followed by Holm-Bonferroni correction): baseline vs. blockade, $Z = -3.1$, $p = 0.002$; blockade vs. recovery, $Z = -2.12$, $p = 0.034$.

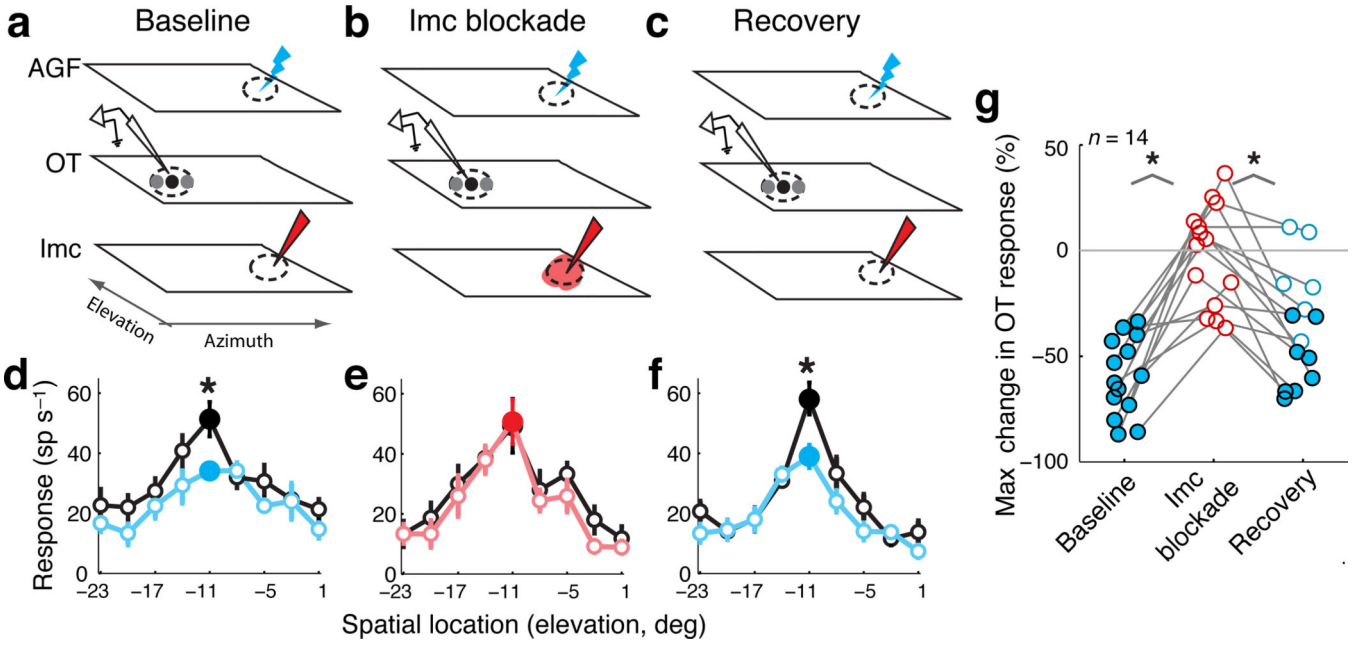

Figure 5. Endogenous competitive inhibition in the OTid abolished by Imc blockade

(a–c) Schematics of the electrode configurations; conventions as in Figure 2a–c. Also shown is the AGF, with the blue lightning bolt signifying the locus of electrical microstimulation in the AGF (endogenous signal).

(d–f) Responses of an OTid unit to the RF stimulus alone (black), or to the RF stimulus paired with AGF microstimulation at a "non-aligned" site (blue or red). Distance between the RFs of the OTid and AGF sites = 34°; distance between the RFs of the AGF site and the site of Imc inactivation = 2.5°. Loom speed of RF stimulus = 5.6 °/s; strength of microstimulation current = 10 μA. Data represent mean ± s.e.m. Filled circles indicate responses to the stimulus location yielding maximal change; '*': $p < 0.05$, t-tests at individual locations followed by Holm-Bonferroni correction ($n = 10$ reps per stimulus condition per location, $df = 18$; Methods).

(g) Population summary of endogenous response suppression in the OTid, based on the maximum suppression obtained during a spatial tuning curve measurement for each unit (circles). Conventions same as in Figure 2m. '*': $p < 0.05$ (paired t-tests followed by Holm-Bonferroni correction): baseline vs. blockade, $t(13) = -6.8$, $p < 0.0001$; blockade vs. recovery, $t(13) = 5.3$, $p = 0.0002$; $n = 14$ units from 5 birds. See also Supplementary Figure 3h.

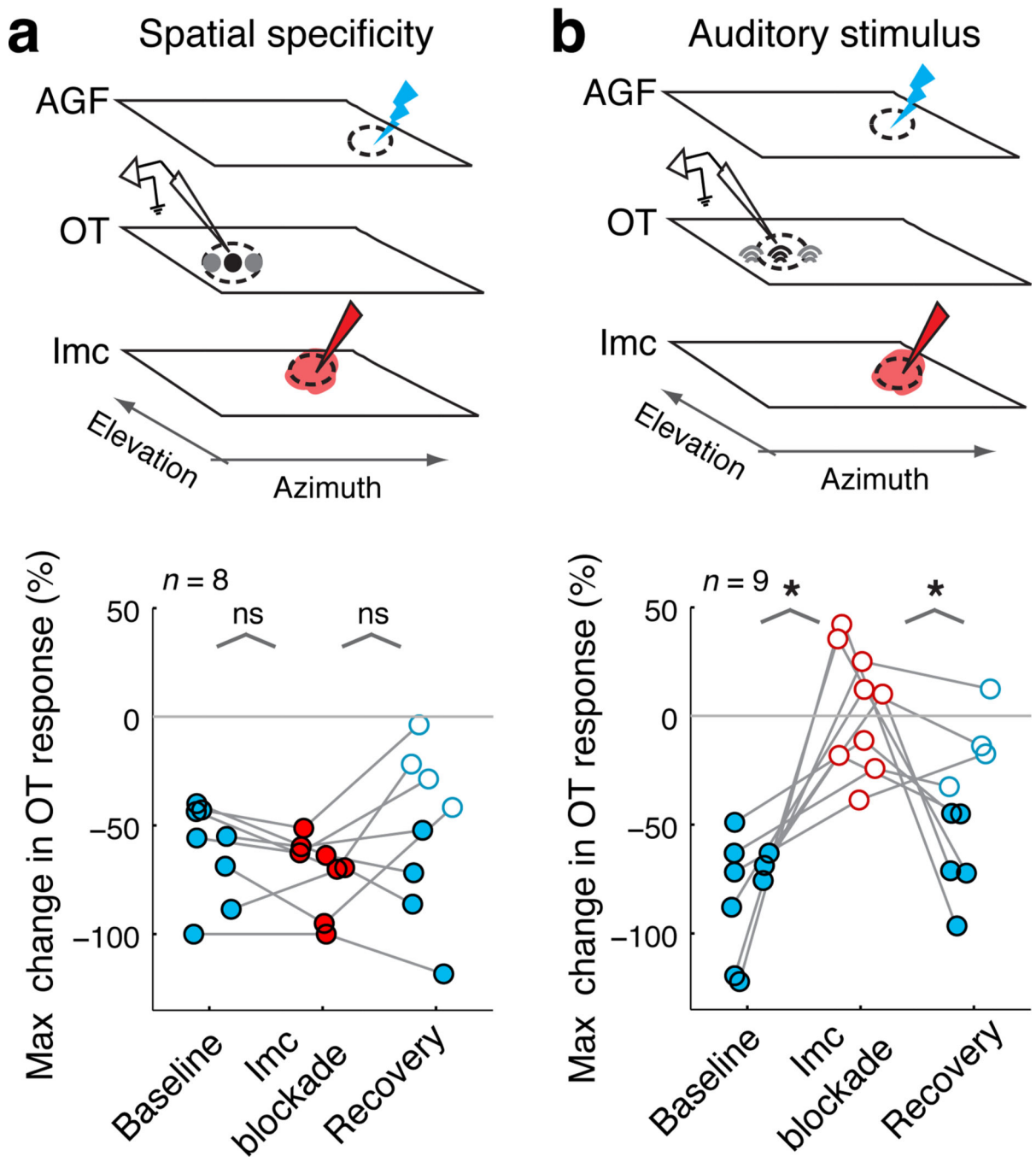

Figure 6. The Imc mediates space-specific, sensory modality independent endogenous competitive inhibition in the OTid

(a) Spatial specificity. *Top panel.* The Imc RF is offset with respect to the AGF site, as well as the OTid site. *Bottom panel*. Population summary of endogenous response suppression in the OTid. Conventions as in Figure 5g, 3a. 'ns': $p > 0.05$ (Mann-Whitney U-tests; small sample size): baseline vs. blockade, $p = 0.20$; blockade vs. recovery, $p = 0.28$; $n = 8$ units from 4 birds.

(b) Sensory modality independence. *Top panel.* Black and gray icons represent the locations of an auditory RF stimulus. *Bottom panel*: Population summary of endogenous response suppression in the OTid. Conventions as in Figure 5g. '*': $p < 0.05$ (Mann-Whitney U-tests followed by Holm-Bonferroni correction): baseline vs. blockade, $p < 0.0001$; blockade vs. recovery, $p = 0.014$; $n = 9$ units from 2 birds. See also Supplementary Figure 4d.